Calculated Performance of Low-Porosity Regenerators at 4 K with He-4 and He-3

R. Radebaugh[1], Y. Huang[2], A. O'Gallagher[1], and J. Gary[1]

[1]National Institute of Standards and Technology
Boulder, CO 80305
[2]Institute of Refrigeration and Cryogenics
Shanghai Jiao Tong University
Shanghai, China

ABSTRACT

Previously we have shown that the lower volumetric heat capacity and more ideal behavior of helium-3 compared with helium-4 at 4 K results in an improved performance for packed sphere regenerators operating with helium-3 between 4 K and 0 K. In this paper we use the NIST numerical software REGEN3.3 to calculate the regenerator loss and the coefficient of performance (COP) of 4 K regenerators with porosities between 0.1 and 0.38 for parallel holes in a rare-earth matrix operating at 30 Hz frequency using either helium-3 or helium-4. A comparison is made with packed spheres at a porosity of 0.38. Calculations were made for average pressures ranging from 0.3 MPa to 1.5 MPa, mostly with a pressure ratio of 1.5. The results show that the regenerator loss decreases and the COP increases as the porosity decreases for all average pressures. For helium-3 the regenerator performance is improved for pressures below 1 MPa, whereas the lower pressures do not benefit helium-4 regenerators. The COP of a helium-3 regenerator with 0.2 porosity operating at 30 Hz and 0.5 MPa average pressure is about 3.8 times higher than a helium-4 regenerator using packed spheres with 0.38 porosity. The effect of regenerator matrix material and the temperature of the heat capacity peak are also investigated.

INTRODUCTION

The application of low temperature superconducting (LTS) systems, such as magnetic resonance imaging (MRI) systems utilizing superconducting magnets or electronic devices utilizing Josephson junctions, requires the use of 4 K cryocoolers. Typically these cryocoolers have been either Gifford-McMahon (GM) cryocoolers, or GM-type pulse tube cryocoolers that operate at frequencies of about 1 Hz.[1] The efficiency of these cryocoolers is in the range of 0.5 to 1.0 % of Carnot, whereas 80 K cryocoolers often achieve efficiencies of about 15 % of Carnot. The low efficiency of 4 K cryocoolers leads to large compressors with large input powers. The low operating frequency of the GM and GM-type pulse tube also leads to large temperature oscillations at the cold end at the operating frequency of the cryocooler. The amplitude of the temperature oscillation decreases as the cryocooler operating frequency is increased. Higher frequencies also allow the use of Stirling cryocoolers or Stirling-type pulse tube cryocoolers, which have much higher efficiencies

Cryocoolers 15, edited by S.D. Miller and R.G. Ross, Jr.

in converting electrical power to PV power. These frequencies are typically in the range of 30 to 60 Hz. However, these higher frequencies generally have lead in the past to greater losses in the regenerator. Recent experiments with a 4 K GM-type pulse tube[2,3] and a Stirling-type pulse tube cryocooler[4] have shown that the use of ^{3}He instead of ^{4}He increased the cooling power for the same power input. Recently we used a new NIST numerical model, REGEN3.3, to calculate the performance of packed-sphere regenerators with the cold end at 4 K using either ^{4}He or ^{3}He as the working fluid.[5] The details of REGEN3.3 are discussed in that paper. We showed that the use of ^{3}He led to losses that are about 15 % lower than that using ^{4}He. Also, the loss at 30 Hz was only slightly higher than that at 1 Hz as long as the regenerator was optimally designed. With packed spheres the porosity is fixed at about 0.38. In this paper we calculate the losses for 4 K regenerators that consist of a set of parallel holes through the matrix. The porosity is varied between 0.1 and 0.38. In most cases the matrix consists of several layers of rare earth materials with high heat capacities. We vary these matrix materials to find the optimum combination.

CRYOCOOLER THERMODYNAMICS

Regenerative cryocooler losses

Only the last-stage regenerator, which reaches 4 K, is considered in the analysis presented here. The time-averaged acoustic power $\{P\dot{V}\}_h$ that drives this stage enters the regenerator at the hot end at a temperature of T_h. It is defined by the reversible isothermal power input given by the time-averaged Gibbs free energy flow $\{\dot{G}\}_h$. The purpose of the regenerator is to deliver as much of this acoustic power to the cold end as possible with a minimum of losses. For Stirling or Gifford-McMahon cryocoolers the displacer at the cold end produces a time-averaged expansion power $\{\dot{W}\}_{\exp}$ that leads to a net refrigeration power given by

$$\dot{Q}_{net} = \langle \dot{W} \rangle_{\exp} - \langle \dot{H} \rangle_{reg} - \dot{Q}_{cond} - \dot{Q}_{rad} \tag{1}$$

where $\{\dot{H}\}_{\exp}$ is the time-averaged enthalpy flow in the regenerator, with positive numbers referring to flow from the warm end to the cold end, $\dot{Q}_{cond}$ is the conduction heat leak through the regenerator, and $\dot{Q}_{rad}$ is the radiation heat leak to the cold end, which is ignored in this work. The expansion power is related to the isothermal reversible power or acoustic power at the cold end $\{P\dot{V}\}_c$ by

$$\langle \dot{W} \rangle_{\exp} = \langle \dot{W} \rangle_{rev} - \dot{Q}_{pt} = \langle P\dot{V} \rangle_c - \dot{Q}_{pt} \tag{2}$$

where $\dot{Q}_{pt}$ is the loss associated with an imperfect pulse tube or any irreversible expansion process at the cold end. The introduction of acoustic power in Equation (2) makes it valid for pulse tube cryocoolers as well as for Stirling and Gifford-McMahon cryocoolers.

The loss associated with the enthalpy flow $\{\dot{H}\}_{\text{reg}}$ in the regenerator can be divided into two parts, as given by

$$\langle \dot{H} \rangle_{reg} = \langle \dot{H} \rangle_P + \dot{Q}_{reg} \tag{3}$$

where $\{\dot{H}\}_P$ is the enthalpy flow associated with the enthalpy pressure dependence (real gas effect) and $\dot{Q}_{reg}$ is the thermal loss associated with enthalpy flow caused by imperfect heat transfer and limited heat capacity in the regenerator (regenerator ineffectiveness). This separation allows us to determine the intrinsic loss associated with using a real gas and how that differs between ^{4}He and ^{3}He. Both gas properties and regenerator properties affect. Combining Equations (1), (2), and (3) gives us

$$\dot{Q}_{net} = \langle P\dot{V} \rangle_c - \langle \dot{H} \rangle_P - \dot{Q}_{reg} - \dot{Q}_{cond} - \dot{Q}_{pt} \tag{4}$$

We can define the gross refrigeration power as that associated with a perfect regenerator and a perfect expansion process, which then gives[5]

$$\dot{Q}_{gross} = \langle P\dot{V} \rangle_c - \langle \dot{H} \rangle_P = \langle P\dot{V} \rangle_c \left[1 - \frac{\langle \dot{H} \rangle_P}{\langle P\dot{V} \rangle_c} \right] \tag{5}$$

Equations (4) and (5) can be combined to give

$$\dot{Q}_{net} = \langle P\dot{V} \rangle_c \left[1 - \frac{\langle \dot{H} \rangle_P}{\langle P\dot{V} \rangle_c} \right] \left[1 - \frac{\dot{Q}_{reg}}{\dot{Q}_{gross}} - \frac{\dot{Q}_{cond}}{\dot{Q}_{gross}} - \frac{\dot{Q}_{pt}}{\dot{Q}_{gross}} \right] \tag{6}$$

The acoustic power anywhere along the regenerator with perfect heat transfer and no pressure drop varies as the specific volume. In the presence of a pressure drop the cold-end acoustic power is related to the hot-end acoustic power by

$$\langle P\dot{V}\rangle_c = \left(Z_c T_c / Z_h T_h\right)\left(\langle P\dot{V}\rangle_h - \langle \Delta P\dot{V}\rangle_h\right) \tag{7}$$

where Z_c is the compressibility factor at the cold end, Z_h is the compressibility factor at the hot end, and $\{\Delta P\dot{V}\}_h$ is the additional acoustic power required at the hot end due to pressure drop in the regenerator. By substituting Equation (7) into Equation (6) we can express the net refrigeration power as

$$\dot{Q}_{net} = \langle P\dot{V}\rangle_h \left[1 - \frac{\langle \Delta P\dot{V}\rangle_h}{\langle P\dot{V}\rangle_h}\right]\left[\frac{Z_c T_c}{Z_h T_h}\right]\left[1 - \frac{\langle \dot{H}\rangle_P}{\langle P\dot{V}\rangle_c}\right]\left[1 - \frac{\dot{Q}_{reg}}{\dot{Q}_{gross}} - \frac{\dot{Q}_{cond}}{\dot{Q}_{gross}} - \frac{\dot{Q}_{pt}}{\dot{Q}_{gross}}\right] \tag{8}$$

By writing the net refrigeration power in this manner, we have separated out the terms that are functions only of the gas properties from those that also depend on the hardware. The first factor on the right hand side of the equation is the acoustic power input at the hot end of the regenerator. The second factor shows the effect of pressure drop in the regenerator and is both hardware and gas dependent. The third factor shows the reduction in acoustic power due to temperature change and real-gas behavior associated with compressibility. The fourth factor shows the effect of real-gas enthalpy flow. The terms in the last set of brackets are both hardware and gas dependent.

Figure 1 shows a schematic of the energy flows and losses associated with the last stage of a regenerative cryocooler as represented by Equation (8). The relative magnitudes shown for each of the acoustic power flows and the losses are typical of a regenerative cryocooler at 4 K. As this figure shows, the losses are quite large and the remaining net refrigeration power is quite small compared to the input power.

Coefficient of performance and efficiency

The coefficient of performance of the last stage regenerator is given by

$$\mathrm{COP} = \frac{\dot{Q}_{net}}{\langle P\dot{V}\rangle_h} \tag{9}$$

For an ideal gas and a perfect regenerator the ideal COP for this last-stage regenerator is given by (T_c/T_h), where we assume that the reversible expansion work at the cold end is not being fed back to the hot end of this regenerator. Thus, the second law efficiency of the last stage is given by

$$\eta = \left(T_h / T_c\right)\mathrm{COP} \tag{10}$$

Combining Equations (8), (9), and (10) gives the second law efficiency of the last stage as

$$\eta = \left[1 - \frac{\langle \Delta P\dot{V}\rangle_h}{\langle P\dot{V}\rangle_h}\right]\left[\frac{Z_c}{Z_h}\right]\left[1 - \frac{\langle \dot{H}\rangle_P}{\langle P\dot{V}\rangle_c}\right]\left[1 - \frac{\dot{Q}_{reg}}{\dot{Q}_{gross}} - \frac{\dot{Q}_{cond}}{\dot{Q}_{gross}} - \frac{\dot{Q}_{pt}}{\dot{Q}_{gross}}\right] \tag{11}$$

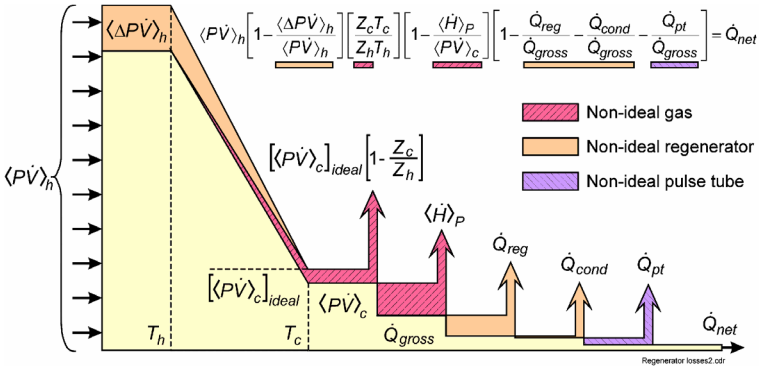

Figure 1. Diagram showing energy flows and losses in a regenerator.

Equation (11) also expresses the ratio of the net entropy input at the cold end $\dot{Q}_{net}/T_c$ to the time-averaged entropy flow at the warm end of the regenerator $\{\dot{S}\}_h$.

REAL GAS EFFECTS

When only the real gas effects are taken into account the net refrigeration power equals the gross refrigeration power, as given by Equation (5). For a perfect regenerator the lost acoustic power due to pressure drop in Equation (7) is zero. The efficiency for a perfect last stage becomes

$$\eta_{gross} = \frac{Z_c}{Z_h}\left(1 - \frac{\langle \dot{H} \rangle_P}{\langle P\dot{V} \rangle_c}\right) \tag{12}$$

The enthalpy flow associated with the real gas effects can be found by using a first law energy balance on the regenerator with perfect isothermal heat exchangers on each end along with the condition that the hot-blow stream must be warmer than the cold-blow stream. Details of this calculation have been discussed previously.[5] Figure 2 compares the efficiency given by Equation (12) for ^{4}He and ^{3}He working fluids. This figure shows that for temperatures below about 7 K ^{3}He gives a much higher gross efficiency than that given by ^{4}He. This figure also shows that for ^{3}He a reduction of the average pressure to about 0.5 MPa significantly increases the efficiency, whereas the lower pressure actually decreases the efficiency slightly at 4 K for ^{4}He.

EFFECT OF GEOMETRY AND POROSITY ON REGENERATOR PERFORMANCE

Regenerator details

Many of the calculations were made on regenerators with a matrix composed of a fictitious material designated Mix 1 in REGEN3.3 that has the specific heat given by a series of several real materials, where the material with the highest volumetric heat capacity at any given temperature is used. Figure 3 shows the volumetric heat capacities of these materials and that used for Mix 1. Once the calculation for Mix 1 is completed with REGEN3.3 and the temperature profile is determined, then the actual regenerator would be made with layers of the separate materials with the interfaces at the locations determined by the temperature profile. Although Fig. 3 shows the heat capacity of gadolinium oxisulfide[6] Gd_2O_2S (GOS), it is not included in Mix 1. Figure 3 also shows the volumetric heat capacity of ^{3}He and ^{4}He for various pressures. We see that ^{3}He has a lower heat capacity than that of ^{4}He, which would suggest that the regenerator loss for ^{3}He should be less than that for ^{4}He. We found previously[7] that the ratio of the regenerator gas volume to the cold-end swept volume is a fundamental parameter that affects the performance of 4 K regenerators operating with ^{4}He working fluid. Because both the conduction and pressure drop are rather small for most 4 K regenerators, the aspect ratio has little influence on the performance, although the regenerators modeled here are close to optimum in aspect ratio. Unless otherwise specified the regenera-

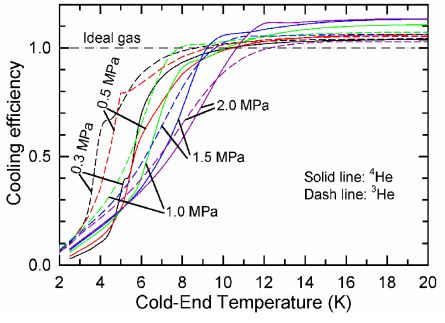

Figure 2. Ratio of real gas COP to ideal gas COP for a perfect last stage of a regenerative cryocooler.

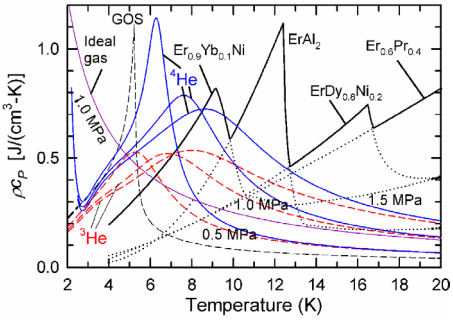

Figure 3. Volumetric heat capacity of regenerator material Mix 1 (heavy line) and its components (dotted line) compared with that of ^{4}He, ^{3}He, and an ideal gas.

tor length was taken as 30 mm. A conductivity degradation factor of 0.3 was used to account for the boundaries in spheres or multiple layers. A frequency of 30 Hz was used for all the calculations reported here. Previous calculations[5] for 1 Hz showed only a small decrease in regenerator loss at the lower frequency.

Calculated regenerator losses

Figure 4 compares the calculated relative regenerator losses for ^{4}He and ^{3}He as a function of the reduced volume ratio, where V_{rg} is the regenerator gas volume and V_E is the swept volume of the expansion space at the cold end. These losses were calculated using REGEN3.3. As expected, the loss with ^{3}He is less than that with ^{4}He. Large regenerator volumes lead to a reduced loss, but for volume ratios of about 10 or higher the phase of the mass flow at the warm end compared with the pressure (shown in Fig. 4 by numbers nest to each data point) becomes rather high and leads to a large compressor swept volume and higher losses in the warmer regenerators that are needed for precooling. Thus, all subsequent calculations discussed here are for volume ratios in the range of about 7 to 10. Although not shown here, we found that varying average pressures between 0.5 MPa and 1.5 MPa has little effect on the regenerator loss. As shown by Equation (8) the net refrigeration power becomes zero when $\dot{Q}_{reg}/\dot{Q}_{gross} = 1$, as long as there is no conduction or pulse tube loss. In the cases analyzed here, the conduction loss is negligible and the pulse tube (expansion) loss is taken as zero. In practice the relative pulse tube or other expansion loss may be about 0.2.

Figure 5 shows the relative regenerator losses for 25 mm diameter parallel holes of porosity 0.38 in Mix 1 for the case of $P_r = 1.5$. These losses are slightly lower than that of packed spheres. The relative similarity of the losses for the two geometries is consistent with the loss being dominated by the limited matrix heat capacity rather than by limited heat transfer coefficient. Parallel holes have a much higher ratio of heat transfer to pressure drop compared with packed spheres. The sphere size and the hole size were close to the optimum value. These hydraulic diameter optimums as well as the optimum for length, area per unit flow, and porosity are determined by maximizing the coefficient of performance for the regenerator, as discussed in the following section.

Calculated coefficient of performance and efficiency

As discussed in a previous section, the product (T_h/T_c)COP of the temperature ratio times the coefficient of performance represents the second law efficiency of the regenerator. This efficiency, as expressed by Equation (11) takes into account real gas losses, regenerator thermal loss, pressure drop loss, and conduction loss in the matrix. The pulse tube or expansion loss is taken as zero for these calculations because it does not represent a loss associated with the regenerator. Figure 6 shows the effect of aspect ratio on the regenerator efficiency in packed spheres for a fixed volume ratio of 9.8 for ^{4}He and 7.7 for ^{3}He. The broad maximum is a result of small conduction and pressure drop losses. The figure also shows the results of two cases where the sphere diameter was

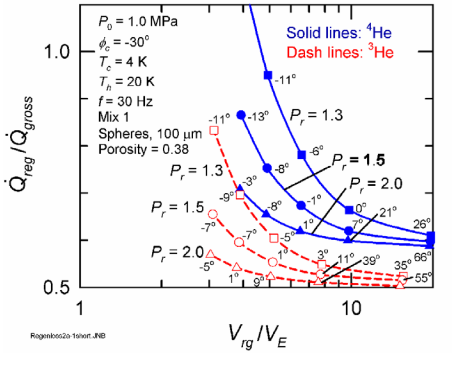

Figure 4. Reduced regenerator loss for packed spheres at three different pressure ratios.

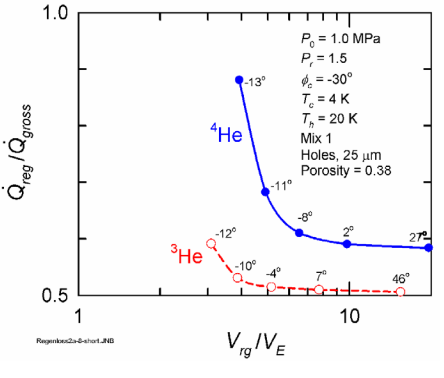

Figure 5. Reduced regenerator loss for parallel holes with 1.5 pressure ratio.

decreased from 100 mm to 80 mm with almost no effect on the loss. Figure 7 shows the effect of aspect ratio in parallel holes, but with a matrix material of GOS + $Er_{0.5}Pr_{0.5}$ instead of Mix 1. This material will be discussed further in a later section. The maximum in COP for the parallel holes is somewhat sharper compared with that for the spheres, but both figures show that a regenerator length of 3 cm is close to the optimum value. This length is chosen for all the following calculations.

Variable porosity with parallel holes

Figure 8 shows the regenerator loss as a function of porosity for the case of parallel holes. As the porosity was decreased, the total cross sectional area was increased to keep the regenerator gas volume and pressure drop constant. However, the conduction loss increases as the porosity is lowered, but it does not become significant until the porosity is less than about 0.15. With a porosity of 0.10 the conduction loss at the midpoint of the regenerator is about 10% of the gross refrigeration power. This figure shows that lower porosities significantly reduce the regenerator loss. The higher loss for ^{4}He regenerators at 0.5 MPa compared with that at 1.0 MPa can be explained by the rather high volumetric heat capacity of ^{4}He at 0.5 MPa (see Fig. 3).

Figure 9 shows the efficiency for the parallel holes as a function of porosity. The efficiencies for packed sphere regenerators of porosity 0.38 are shown for comparison. We note that the dramatic reduction in regenerator loss at lower porosities shown in Fig. 8 does not lead to such significant increases in efficiencies at the low porosities. Such behavior can be explained by noting that in Equation (11) when becomes small compared to 1, it has little effect on the value within those brackets, but the real gas contribution in the two preceding sets of brackets primarily determines the efficiency, which is not influenced by the porosity.

The most striking aspect about Fig. 9 is the significantly higher efficiencies shown for ^{3}He at lower pressures. This behavior is consistent with the high efficiency associated with real gas effects shown in Fig. 2 for ^{3}He at 0.3 and 0.5 MPa for 4 K. The disadvantage of using such low pressures is that the swept volume of the compressor becomes rather large for a fixed power input. It would be offset somewhat by the ability to use less input power for the same refrigeration power because of the higher efficiency at these low pressures. Also, these low pressures are not the optimum for high efficiency in the warmer regenerators, although the optimum in the warmer regenerators is a rather weak function of the average pressure.

EFFECT OF MATRIX MATERIAL ON REGENERATOR PERFORMANCE

Matrix heat capacities

The set of materials in the layered Mix 1 has the volumetric heat capacity as given in Fig. 3. Its heat capacity at 4 K is significantly less than that of both ^{4}He and ^{3}He. The relatively new material,

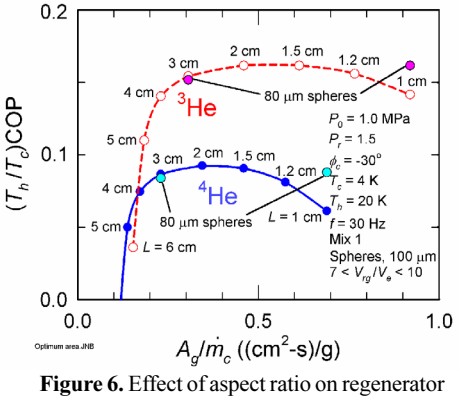

Figure 6. Effect of aspect ratio on regenerator efficiency for fixed volume with packed spheres of Mix 1.

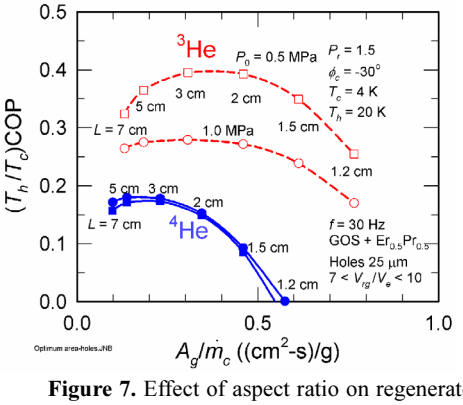

Figure 7. Effect of aspect ratio on regenerator efficiency for fixed volume with parallel holes of GOS + $Er_{0.5}Pr_{0.5}$.

gadolinium oxisulfide[6] Gd_2O_2S (GOS), has a very high heat capacity around 4 K and would be expected to improve regenerator performance. Also, some of the materials in Mix 1 are not commercially available at this time. Therefore, we carried out several calculations with both spheres and parallel holes where only the matrix material was varied. In all cases the calculations for more than one material are carried out in the same manner as performed for Mix 1 in which the highest heat capacity is always used at any given temperature.

Figure 10 shows the volumetric heat capacities of matrix materials used in the calculations to follow. These heat capacities are compared with that of ^{4}He and ^{3}He at various pressures. All of the materials shown in this figure are commercially available at this time.

Comparison of regenerator performance with different materials

The calculations described in this section were made on regenerators operating at 30 Hz with an average pressure of 0.5 MPa. For spheres the particle diameter was 100 mm with a porosity of 0.38. The hydraulic diameter is then 40.9 mm. For the case of the parallel holes the hole diameter and hydraulic diameter was 25 mm and the porosity was 0.2. For both geometries the length was 30 mm and the volume ratio V_{rg}/V_E was 9.2 for ^{4}He and 6.5 for ^{3}He. Such ratios gave nearly the same warm end phase angle between flow and pressure that ranged from about 0 to 15 degrees, depending on the regenerator matrix material.

Figure 11 shows the relative regenerator loss for spheres of different materials, and Fig. 12 shows the regenerator efficiency for spheres of the different materials. The loss and efficiency for parallel holes are shown in Figs. 13 and 14. There are several interesting features of these comparisons. First, the loss for Mix 1 is relatively high compared with other materials that have higher volumetric heat capacities very near 4 K. Second, for the case of spheres with GOS + Pb the relative loss for ^{3}He is higher than that for ^{4}He. That is the only case where such behavior occurs. Third, the addition of $ErNi_{0.9}Co_{0.1}$ to the GOS + $Er_{0.5}Pr_{0.5}$ mix increases the loss even though it contributes a higher heat capacity in the valley region between that of GOS and $Er_{0.5}Pr_{0.5}$. At this time we have no explanation for the second and third feature. Finally, the efficiency of a parallel hole regenerator of GOS + $Er_{0.5}Pr_{0.5}$ using ^{3}He is about five times that of a sphere regenerator made with Mix 1 or ErNi using ^{4}He. When comparing only the case of ^{3}He working fluid, the holes in GOS + $Er_{0.5}Pr_{0.5}$ give an efficiency about twice that of spheres of Mix 1 or ErNi.

CONCLUSIONS

We have shown that the thermodynamic properties of ^{3}He are such that when it is used as the working fluid in a 4 K perfect regenerative cryocooler, the efficiency will be higher than one using ^{4}He as long as the average pressure is less than about 1.5 MPa. For 4 K operation lower average pressures lead to higher real gas efficiencies for the case of ^{3}He. An average pressure of about

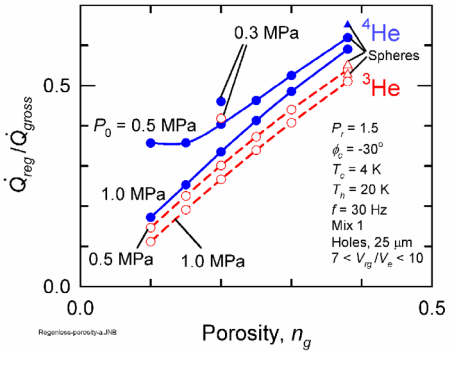

Figure 8. Reduced regenerator loss as a function of porosity for parallel holes.

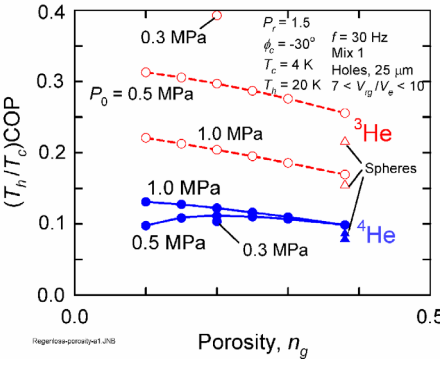

Figure 9. Regenerator efficiency as a function of porosity for parallel holes.

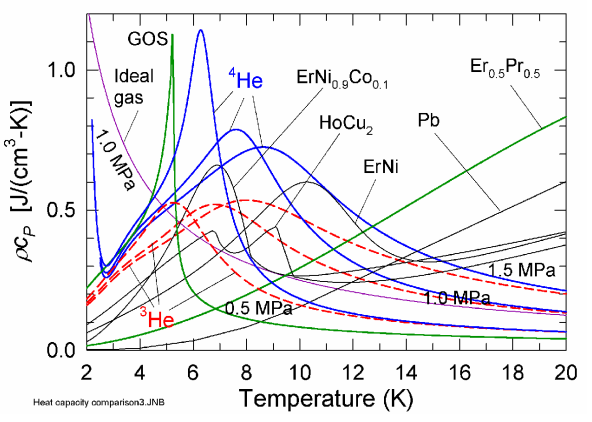

Figure 10. Volumetric heat capacity of various regenerator materials investigated here compared with that of ^{4}He and ^{3}He at various pressures.

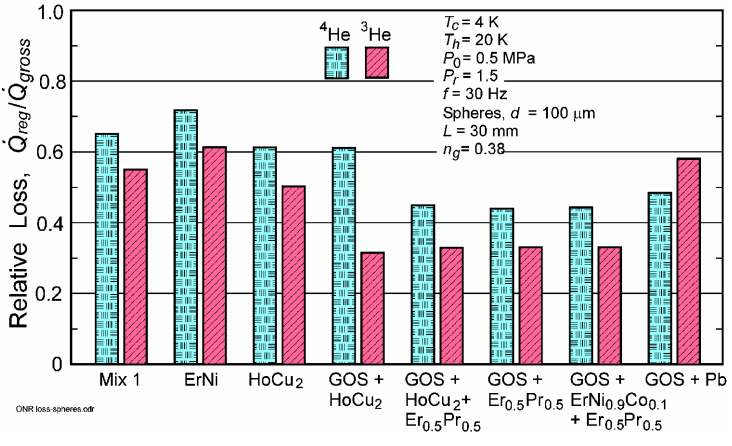

Figure 11. Relative regenerator loss for spheres of various regenerator materials

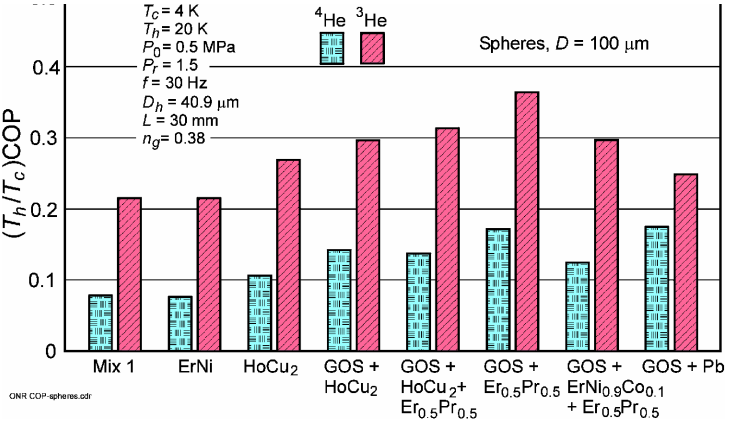

Figure 12. Regenerator efficiency for spheres of various regenerator materials

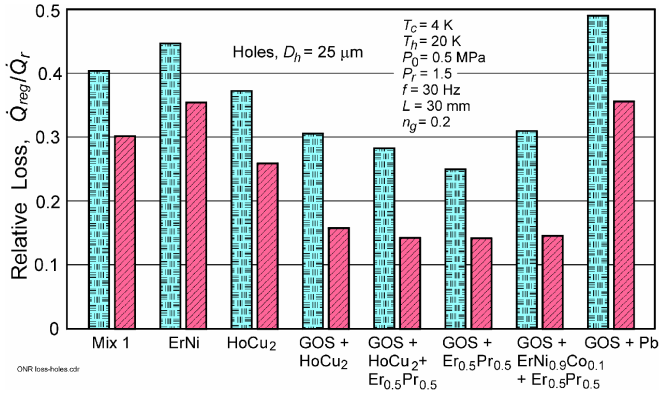

Figure 13. Relative regenerator loss for parallel holes in various regenerator materials.

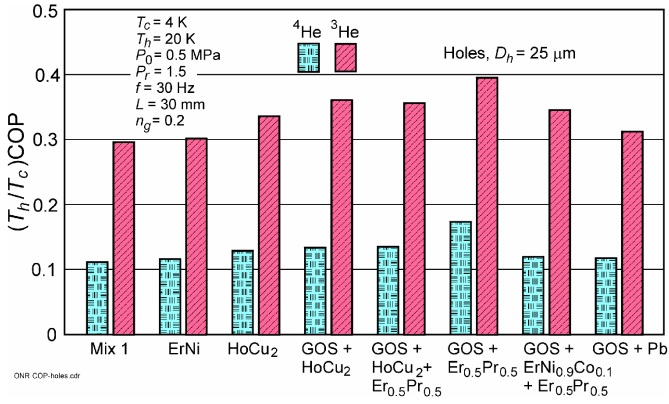

Figure 14. Regenerator efficiency for parallel holes of various regenerator materials.

0.5 MPa is shown to be near an optimum value. The relative regenerator loss for parallel holes of porosity 0.38 is only slightly less than that of packed spheres with the same porosity. As the porosity is lowered to 0.1 the regenerator loss decreases approximately proportional to the porosity and becomes small compared to 1. However, the regenerator efficiency, given by (T_h/T_c)COP increases only slightly for porosities less than about 0.20 because the real gas losses dominate that caused by the real regenerator at such low porosities. In comparing eight different regenerator matrix materials, we found that the layered combination of GOS + $Er_{0.5}Pr_{0.5}$ gives the lowest regenerator loss and highest regenerator efficiency. That material combination gives 1.8 to 2.0 times higher efficiency compared with the same regenerator made with Mix 1 or ErNi. With a GOS + $Er_{0.5}Pr_{0.5}$ regenerator the efficiency with low porosity parallel holes is only slightly higher than that with 0.38 porosity packed spheres for both ^{4}He and ^{3}He. However, the efficiency increases by a factor of two when ^{4}He is replaced with ^{3}He in the same regenerator. The regenerator efficiency of parallel holes of GOS + $Er_{0.5}Pr_{0.5}$ at a porosity of 0.2 in ^{3}He is about five times that of packed spheres of Mix 1 or ErNi at a porosity of 0.38 in ^{4}He. Such a large increase in efficiency is an example of what can be achieved by the optimization of all the factors involved in the performance of 4 K regenerators. The large gains in efficiency discussed here pertain only to the last stage regenerator in a 4 K regenerative cryocooler. Calculations for the entire cryocooler are needed to determine the gain in the overall cryocooler efficiency when making the improvements discussed here. However, because entropy losses in the last regenerator stage are quite high, the efficiency gain for the overall cryocooler should still be rather large when using such improved regenerators.

ACKNOWLEDGMENT

This research was partially funded by the Office of Naval Research with Deborah Van Vechten as the project monitor.

REFERENCES

1. Radebaugh, R., "Refrigeration for Superconductors," *Proc. IEEE, Special Issue on Applications of Superconductivity*, vol. 92, (2004), pp. 1719-1734.
2. Xu, M.Y., de Waele, A.T.A.M., and Ju, Y.L., "A pulse tube refrigerator below 2 K," *Cryogenics,* Vol.39, Issue: 10, October 1999, pp. 865-869
3. Jiang, N., Lindemann, F., Giebeler, F., and Thummes, G., "A ^{3}He pulse tube cooler operating down to 1.3 K," *Cryogenics,* Vol. 44, Issue: 11, November 2004, pp. 809-816.
4. Nast, T., Olson, J., Roth, E., Evtimov, B. Frank, D., and Champagne, P., "Development of Remote Cooling Systems for Low-Temperature, Space-Borne Systems," *Cryocoolers 14*, ICC Press, Boulder, CO (2007), pp. 33-40.
5. Radebaugh, R., Huang, Y., O'Gallagher, A., and Gary, J., "Calculated Regenerator Performance at 4 K with Helium-4 and Helium-3," *Adv. in Cryogenic Engineering*, Vol. 53, Amer. Institute of Physics, Melville, NY (2008), pp. 225-234.
6. Numazawa, T., Yanagitani, T., Nozawa, H., Ikeya, Y., Li, R., and Satoh, T., "A New Ceramic Magnetic Regenerator material for 4 K Cryocoolers," *Cryocoolers 12*, Kluwer Academic/Plenum Publishers, New York (2003), pp. 473-481.
7. Radebaugh, R., O'Gallagher, A., and Gary, J., "Regenerator behavior at 4 K: Effect of volume and porosity," *Adv. in Cryogenic Engineering*, Vol. 47B, Amer. Institute of Physics, Melville, NY (2002), pp. 961-968.